NATIONAL AIR INTELLIGENCE CENTER
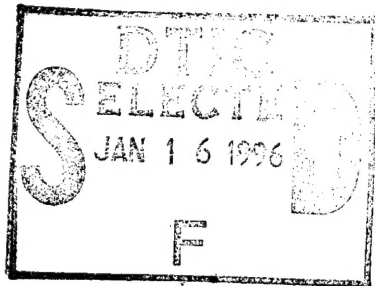
SIMULATIONS ON CONJUGATION FIELD USING DEFORMABLE MIRRORS

by

Fu Changming, Lu Lixin, Sun Jingwen

19960104 006

1

HUMAN TRANSLATION

GRAPHICS DISCLAIMER

All figures, graphics, tables, equations, etc. merged into this translation were extracted from the best quality copy available.

I. INTRODUCTION

T.J. Karr put forward methods associated with the use of two deformable mirrors (DM) to realize field conjugation, improving on typical phase compensation adaptive optics concepts [1]. Control algorithms associated with how, on the basis of second DM light strength distributions, to determine the phase distributions that should be possessed by the first DM are the key to this method. Karr presents "small signal algorithms" appropriate for use with uniform strength light sources. Basically, these only possess theoretical significance. Actual light sources very seldom possess uniform strength. If one wants to make practical applications, it is necessary to study more universally applicable algorithms associated with considerations of light source strength distributions. What most lasers transmit are Gaussian light beams. Therefore, doing research on control algorithms with Gaussian strength distributions is the most practical thing.

II. THEORETICAL ANALYSIS

With a view toward simplicity and convenience, we discuss one dimensional problems. The methods are capable of direct generalization to two dimensional forms.

In vaccuums, near axis electromagnetic wave motion equations are

$$2ik\frac{\partial E}{\partial z} + \nabla_\perp^2 E = 0 \tag{1}$$

Here, k=2π/λ is the wave number. λ is wave length.
Let

$$E = E_0 \exp\{\varphi\},$$
$$\varphi = \chi + i\Phi \tag{2}$$

χ is field logarithmic amplitudes. Φ is phase. Eo is a constant electromagnetic field.
φ satisfies:

$$2ik\frac{\partial \varphi}{\partial z} + \nabla_\perp^2 \varphi + (\nabla_\perp \varphi)^2 = 0 \tag{3}$$

Acting as a very rough estimate, with regard to standard Gaussian light beams, the expression for optical waist positions φ is

$$\varphi = -\frac{x^2}{\omega_0^2}$$

In order to make approximate comparisons with $(\nabla_\perp \varphi)^2$ and $\nabla_\perp^2 \varphi$.

On axses, at x=y=0 locations, $(\nabla_\perp \varphi)^2/(\nabla_\perp^2 \varphi) = 0$
At $|x| = \omega_0/\sqrt{2}$ locations, are on axis strengths of

$$(\nabla_\perp \varphi)^2 / (\nabla_\perp^2 \varphi) = 1$$

With regard to Gaussian light beams, energies are primarily concentrated in the vicinity of light beam centers. Acting as a preliminary analysis, we first ignore $(\nabla_\perp \varphi)^2$, , making linearized equation:

$$2ik \frac{\partial \varphi}{\partial z} + \nabla_\perp^2 \varphi = 0 \qquad (4)$$

Taking ϕ and doing Fourier transforms:

$$\varphi_\kappa = \int_{-\infty}^{+\infty} \varphi(x) \exp(-i\kappa x) dx \qquad (5)$$

Moreover, note $\varphi_\kappa = \chi_\kappa + i\Phi_\kappa$

Substituting in (4), it is possible to obtain:

$$2ik \frac{\partial \varphi_\kappa}{\partial z} - \kappa^2 \varphi_\kappa = 0 \qquad (6)$$

Solving, one gets: $\varphi_\kappa(z) = \varphi_\kappa(0) \exp(-i \frac{\kappa^2 z}{2k})$

代入 (5) 式，$z=z$ 处的场可用 $z=0$ 处的场表示为:

$$(7)$$

Substituting into equation (5), as far as z = z location fields are concerned, it is possible to use z = O location fields expressed as:

$$\varphi(z) = \int_{-\infty}^{+\infty} \varphi_\kappa(0) \exp(-i \frac{\kappa^2 z}{2k}) \exp(i\kappa x) d\kappa \qquad (8)$$

Comparing real parts:

$$\chi(z) = \int_{-\infty}^{+\infty} \{ [\chi_\kappa(0) \cos \frac{\kappa^2 z}{2k} + \Phi_\kappa(0) \sin \frac{\kappa^2 z}{2k}] \cos \kappa x$$

$$+ [\chi_\kappa(0) \sin \frac{\kappa^2 z}{2k} - \Phi_\kappa(0) \cos \frac{\kappa^2 z}{2k}] \sin \kappa x) d\kappa \qquad (9)$$

At z = O locations, one has

$$\chi(0) = \int_{-\infty}^{+\infty} \{ \chi_\kappa(0) \cos \kappa x - \Phi_\kappa(0) \sin \kappa x \} d\kappa \qquad (10)$$

联立 (9)、(10) 式，可得:

Setting up equations (9) and (10) simultaneously, it is possible to obtain:

$$\chi_\kappa(0) = \mathrm{Re}[F(\chi(0))] + \frac{\mathrm{Im}[F(\chi(z))] - \mathrm{Im}[F(\chi(0))]\cos\frac{\kappa^2 z}{2k}}{\sin\frac{\kappa^2 z}{2k}} \tag{11}$$

$$\Phi_\kappa(0) = \mathrm{Im}[F(\chi(0))] + \frac{\mathrm{Re}[F(\chi(z))] - \mathrm{Re}[F(\chi(0))]\cos\frac{\kappa^2 z}{2k}}{\sin\frac{\kappa^2 z}{2k}} \tag{12}$$

/286

In the equations above, F stands for Fourier transform. Ré and Im respectively stand for the real and imaginary parts of adopted functions. Because of this, from equation (5), one knows that, through equations (11) and (12), phases on initial planes are capable of using exponential amplitudes on transmission planes and receiving planes to be represented as:

$$\Phi(0) = \mathrm{Im}\int_{-\infty}^{+\infty} [\chi_\kappa(0) + i\Phi_\kappa(0)]\exp\{i\kappa x\}dk = \mathrm{Im}[F^{-1}(\chi_\kappa(0) + i\Phi_\kappa(0))] \tag{13}$$

F-1 stands for Fourier reverse transforms.

III. NUMERICAL VALUE SIMULATION RESULTS AND DISCUSSION

Under conditions which satisfy $(\nabla_\perp\varphi)^2 \ll \nabla_\perp^2\varphi$, formula (13) is universally applicable. Here, numerical value simulations are only carried out with regard to Gaussian light beams.

The basic steps associated with numerical value simulations are as follows. First, from the law of conservation of energy, one gets a rational target reception field strength distribution. Second, from equation (13), one constructs phase distributions on transmission planes. Then, from Fresnel diffractive integration formulae, calculations are done of diffractive strength distributions on second DM. Comparing differences between these and required fields, empirical verification is done of the feasibility of algorithms. Numerical value simulation results are given below.

We adopt wave length λ = 1 micron. Curve 1 is transmission field Gaussian strength distribution. Curve 2 is the strength distribution required on second DM. Curve 3 is a phase distribution produced in association with equation (13). Curve 4

is optical strengths obtained in association with diffraction integrals.

First of all, we carried out numerical value simulations with regard to required strengths having sine distribution forms. The results were as shown in Fig.1. The produced strengths and the required strengths are basically in agreement. Because, in the case of any curve, it is possible to see forming--in all situations--a series of sine and cosine functions superimposed on each other, this special case possesses universal significance.

In order to avoid irrational situations where one has the appearance of negative values in association with required strengths given, the required strength distributions below are given in this way. From the law of the conservation of energy, one is given a Gaussian strength distribution with an optical waist larger than the optical waist of the original light source. Then, in the logarithmic amplitudes, sine and cosine perturbations are brought to bear.
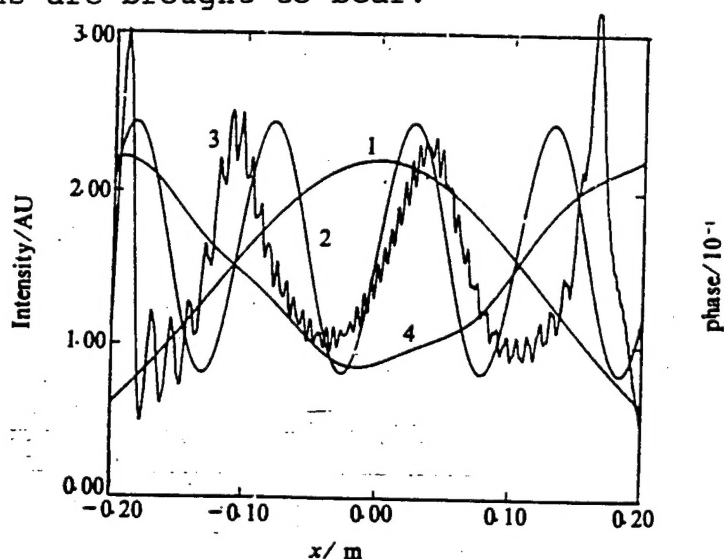
Fig.1

Fig.1 Simulation on sine-shaped target intensity pattern

$D = 0.4m, \omega_o = 0.25m, z = 1000m$

Fig.2 is numerical value simulation results when $D = 0.4m$, $\omega o = 0.25m$, and $z = 1000m$. Due to errors associated with machines and algorithms themselves, transmission field phases given by equation (13) are made very rough. Moreover, they carry with them small local oscillations, leading to abrupt local oscillations of diffraction strengths.

What is fortunate is that deformable mirrors are very smooth. They are capable of automatically getting rid of small
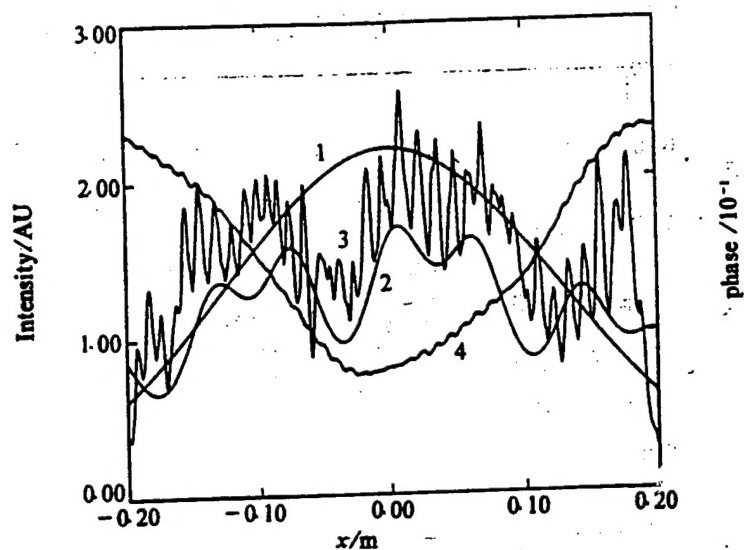
84

Fig.2 Voilent shake of intensity on the second DM resulted from the slight local fluctuation.
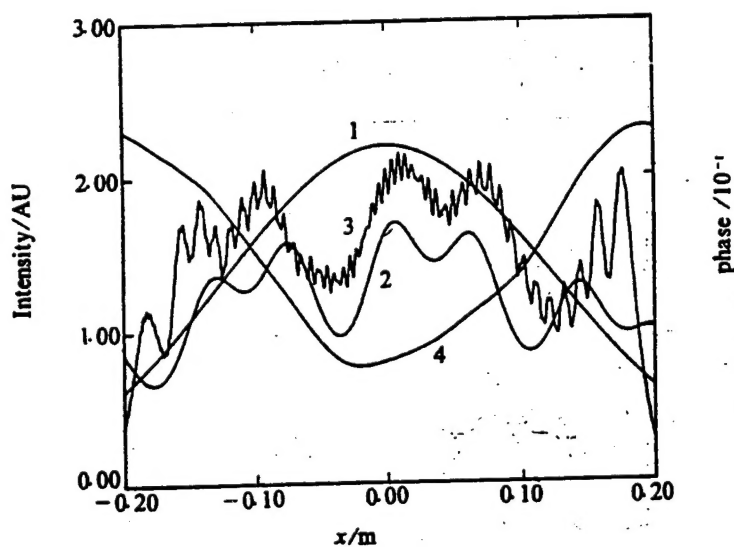$D=0.4m$, $\omega_{\bullet}=0.25m$, $z=1000m$

Fig.2

Fig.3 The intensity pattern on the second DM is distinctly improved after the local phase fluctuations on the first DM is deprived by fitting the phase using spline function.
$D=0.4m$, $\omega_{\bullet}=0.25m$, $z=1000m$

Fig.3

/289

local phase perturbations thereby improving diffraction strength distributions. Deformable mirror surfaces (or phase distribution) third (illegible) degree spline functions are the most appropriate for description. Making comparisons with Fig.2, Fig.3 presents centers deviated relatively more from required/289 fields. Paying attention to increases in $(\nabla_\perp\varphi)^2/\nabla_\perp^2\varphi$ values along transverse distances, we estimate that the deviations discussed above are caused due to the ignoring of $(\nabla_\perp\varphi)^2$ terms in equation (4).

What makes people pleasantly surprised is that, although diffraction strength distributions are very complicated, phase change ranges are also relatively large ($\sim 8\pi$). However, phase curve forms are still quite simple. This is extremely advantageous to deformable mirrors accurately structuring phases. This is one big advantage of Gaussian light beams acting as light sources.
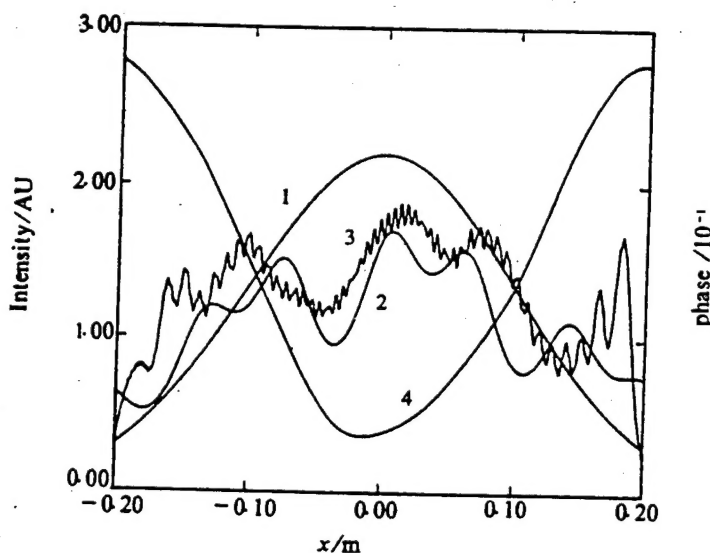
Fig.6

Fig.6 The intensity pattern when $\omega_0 = D/2$, $D = 0.4\text{m}$, $\omega_0 = 0.20\text{m}$, $z = 1000\text{m}$

Fig.5 is numerical value simulation results when $\omega o = 0.15\text{m}$. Comparisons with Fig.3 clearly show that the larger $D/2\omega o$ is, the worse results are. The reason still lies in ignoring $(\nabla_\perp\varphi)^2$. From comprehensive consideration of the two areas of energy utilization rates and precision, taking $D/2\omega o = 1$ is relatively appropriate. In this type of situation, Fig.6 gives results ($\omega o = 0.2\text{cm}$).
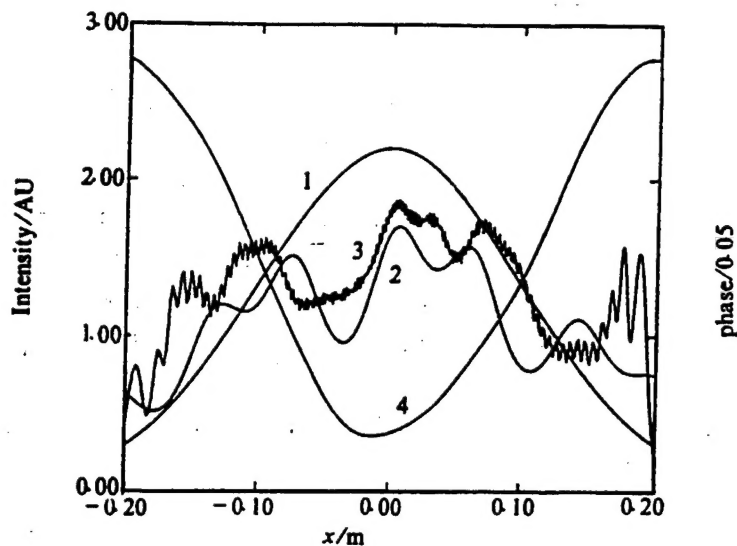
Fig . 7   The shorter distance between the two DMs requires larger phase performance range of the first DM.

Fig.7

Fig.7 is simulation results when the distance between the two DM is z = 500m.   Comparisons with Fig.6 clearly show that, taking z and shortening it one fold, it is then necessary to make deformable mirror dynamic ranges increase one fold.   In actual applications, appropriate distances between the two DM will finally be determined by various types of factors such as target strengths as well as deformable mirror operating ranges, and so on.

To summarize what has been said above, numerical value simulations clearly show that this type of algorithm is definitely capable of structuring appropriate phase distributions, basically obtaining required target strength distributions.   However, ignoring $(\nabla_{\perp}\varphi)^2$ introduced a certain error.   In particular, at places where transverse distances are relatively large, errors are not easy to ignore. Considering the influence of $(\nabla_{\perp}\varphi)^2$, it is possible to more accurately produce the needed strength distributions.   We will carry out further probes of this later on.

Besides algorithms needing further improvement, there exist certain problems with plans themselves.   As far as deformable mirrors are concerned, although capable of getting rid of the influences of small local phase perturbations, local strength oscillations created by diffraction, however, are still unavoidable.   With regard to increasing deformable mirror dimensions, it is possible to make diffraction strengths even smoother.   However, this will increase technical difficulties and costs.   The influences of local strength oscillations on

atmospheric transmission are so large that it is necessary to make detailed probes of such questions as whether or not they can be gotten rid of by the wind.

REFERENCES

[1]   Karr TJ. Instabilities of atmospherie laser propagation. Propagation of High Energy Laser Beams through the Atomsphere. *SPIE* 1990, **1221**: 25 − 57.

DISTRIBUTION LIST

DISTRIBUTION DIRECT TO RECIPIENT

ORGANIZATION	MICROFICHE
BO85 DIA/RTS-2FI	1
C509 BALL0C509 BALLISTIC RES LAB	1
C510 R&T LABS/AVEADCOM	1
C513 ARRADCOM	1
C535 AVRADCOM/TSARCOM	1
C539 TRASANA	1
Q592 FSTC	4
Q619 MSIC REDSTONE	1
Q008 NTIC	1
Q043 AFMIC-IS	1
E404 AEDC/DOF	1
E410 AFDTC/IN	1
E429 SD/IND	1
P005 DOE/ISA/DDI	1
1051 AFIT/LDE	1
PO90 NSA/CDB	1

Microfiche Nbr: FTD95C000780
NAIC-ID(RS)T-0515-95